NOTES AND CORRESPONDENCE

Water Mass Transformation and Formation in the Labrador Sea

PAUL G. MYERS

Department of Earth and Atmospheric Sciences, University of Alberta, Edmonton, Alberta, Canada

CHRIS DONNELLY

Department of Earth and Atmospheric Sciences, University of Alberta, Edmonton, Alberta, Canada

(Manuscript received 10 October 2006, in final form 7 August 2007)

ABSTRACT

Objectively analyzed surface hydrographic fields and NCEP–NCAR reanalysis fluxes are used to estimate water mass transformation and formation rates in the Labrador Sea, focusing on Labrador Sea Water (LSW). The authors estimate a mean long-term transformation of between 2.1 ± 0.2 and 3.9 ± 0.3 Sv (Sv $\equiv 10^6$ m^3 s^{-1}) over the years 1960–99 to water with densities greater than $\sigma = 27.65$ kg m^{-3}, depending on the correction used for the latent and sensible heat fluxes. Mean long-term formation rates are found between 0.9 ± 0.2 and 1.7 ± 0.3 Sv for $\sigma = 27.675 - 27.725$ kg m^{-3} and 1.2 ± 0.2 and 2.0 ± 0.3 Sv for $\sigma > 27.725$ kg m^{-3}. There is tremendous variability associated with these formation rates with years of strong water formation (5.7–6.6 ± 0.5–0.7 or 9.5–10.8 ± 0.7–1.1 Sv) mixed with years of little or no formation in the given density ranges. The North Atlantic Oscillation (NAO) is linked (correlation coefficient of 0.45, significant at the 99% level) with the overall formation rate for $\sigma > 27.625$ kg m^{-3}. The observed long-term increase in net precipitation over the Labrador Sea does not seem to have had any significant effect on LSW, potentially reducing LSW transformation rates by 0.1 Sv. A reduction in surface salinity leads to formation occurring at a reduced density, but with little change in the amount of water transformed.

1. Introduction

Located between eastern Canada, the Canadian Arctic, and Greenland, the Labrador Sea is a northern arm of the North Atlantic Ocean (Fig. 1). Shaped as a large bowl open to the south, it is flanked by continental shelves, narrow along Greenland and wider along the Labrador coast. Along these shelves and over the shelf breaks flow the West Greenland Current, the Baffin Island Current, and the Labrador Current, linking the large-scale cyclonic circulation of the region. Associated with cold winds blowing off the continent, convection and deep sinking to 1500–2000 m occur in many winters, offshore of the Labrador Current around 56°–58°N, 52°–55°W (Clarke and Gascard 1983). The resulting water mass is Labrador Sea Water (LSW), which is dispersed through the North Atlantic and whose formation plays a role in the lower limb of the global overturning circulation (The Lab Sea Group 1998). Haine et al. (2008) have recently summarized studies and estimates of LSW formation using a number of approaches. As they discuss (Haine et al. 2008), depending on the period studied, the approach used (hydrography, surface fluxes, tracers, models), as well as the definitions used for LSW and formation rate, the estimates vary widely.

One method used to estimate water formation rates (whether for LSW or other water masses) is based upon a water mass diagnostic approach and the surface buoyancy fluxes. These fluxes help determine the surface density as well as producing water masses of given properties. Thus, given the surface properties as well as buoyancy fluxes, one can determine the formation rate

Corresponding author address: Paul G. Myers, Department of Earth and Atmospheric Sciences, University of Alberta, Edmonton, AB T6G 2E3, Canada.
E-mail: pmyers@ualberta.ca

DOI: 10.1175/2007JCLI1722.1

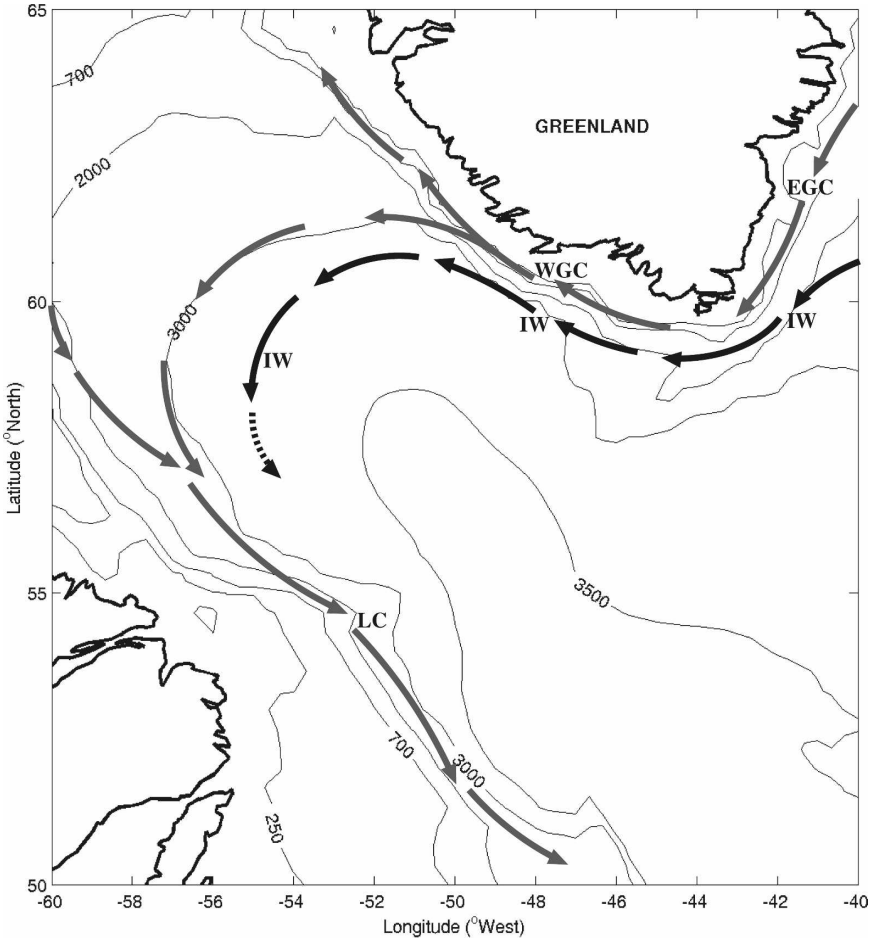

FIG. 1. A map of the Labrador Sea, our study region. The abbreviations used are EGC: East Greenland Current, WGC: West Greenland Current, LC: Labrador Current, and IW: Irminger Water.

of a given water mass in a specified density range. This idea was first expounded upon by Walin (1982) in terms of temperature and heat fluxes and then expanded more generally in terms of density by Tziperman (1986).

Speer and Tziperman (1992) used this approach to estimate the conversion rates of North Atlantic water masses from several air–sea flux sources. They suggested that about 32.2 Sv (Sv $\equiv 10^6$ m^3 s^{-1}) of water are transformed to densities greater than $\sigma = 26.1$ kg m^{-3} each year, associated with a strong subtropical to subpolar gyre transfer. By then looking at the distribution over density of the water mass transformation rate, they showed a peak in formation rate associated with Sub-Polar Mode Water, although the density maximum was low for LSW (traditionally $\sigma = 27.74 - 27.80$ kg m^{-3}). Speer et al. (1995) then extended this work to use fluxes from the Comprehensive Ocean–Atmosphere Dataset. Focusing on the marginal North Atlantic seas, they found only weak wintertime formation section of ~1 Sv in the Labrador Sea, mainly driven by thermal forcing. Using the same method, National Centers for Environmental Prediction–National Center for Atmospheric Research (NCEP–NCAR) reanalysis fluxes and Levitus climatological surface water properties, Khatiwala et al. (2002) suggested that the maximum transformation of LSW has varied between 1.3 and 6.1 Sv (their Fig. 16) with mean formation rates over the density range $\sigma = 27.7 - 27.9$ kg m^{-3} of 2.7 Sv [although sensitive to the surface fluxes used, e.g., they found a mean formation rate of 1.7 Sv using da Silva et al. (1994) fluxes]. This method has also been used in the Mediterranean by Lascaratos (1993) and Tziperman and Speer (1994) and the Nordic seas by Isachsen et al. (2007). Marsh (2000) diagnosed an annual-mean surface-forced streamfunction for the North Atlantic thermohaline circulation and estimated a mean formation for LSW of 3.4 Sv for 1980–97.

Part of the reason for the discrepancy between estimates of LSW formation rates may be that the Labrador Sea has undergone significant variability on interannual to interdecadal time scales and different authors analyzed different regions and periods. Temporal variability may be linked to atmospheric forcing such as changes in heat fluxes due to the North Atlantic Oscillation (NAO; Dickson et al. 1996; Greatbatch 2000; Curry and McCartney 2001), as well as precipitation changes (Josey and Marsh 2005; Myers et al. 2007a), terrestrial effects such as changes in river runoff (Déry et al. 2005), melt from Greenland (Steffen et al. 2004), and oceanic advection events such as Great Salinity Anomalies (GSA; Dickson et al. 1988; Belkin et al. 1998). Additionally, a long-term freshening has been observed for the Labrador Sea, as well as the rest of the subpolar gyre (Dickson et al. 2002; Curry et al. 2003; Curry and Mauritzen 2005). A summary of the recent changes to the Labrador Sea can be found in Yashayaev (2007). Some, but not all authors, in fact argue that the variability in LSW properties is large enough to make it worthwhile to break down the continuum of LSW into two types associated with different density classes [see Haine et al. (2008) for a more detailed discussion of this issue]. This includes the "historical" LSW definition with density of $\sigma = 27.74 - 27.80$ kg m^{-3} (even if the formation of this dense mode is now known to be an occasional event) as well as an upper LSW, first named by Pickart et al. (1996), with density of $\sigma = 27.68 - 27.74$ kg m^{-3} (note that a lower limit of 27.72 was used by Pickart et al. when they first defined this water mass).

Although, as discussed above, formation rates of LSW based upon water mass diagnostics have been examined in previous studies, we decided to reexamine this question for a number of reasons. As Haine et al. (2008) discuss, great progress has been made over the past decade in providing improved estimates of LSW formation rate and its variability: yet the discrepancies between many of these estimates suggest that further work is needed on this topic. Other than the study of Khatiwala et al. (2002), none of the previous studies using this approach focused on the Labrador Sea. In their study, Khatiwala et al. used sea surface density computed from the global climatology of Levitus (Levitus and Boyer 1994; Levitus et al. 1994), whose fields are quite smooth. As accurate surface density fields are as important to estimates of water mass transformation rates as the surface fluxes, we wanted to be able to take into account the detailed hydrography of this basin, including the sharp division of properties from the fresh and cold boundary currents and the warm and relatively salty interior that was not possible in previous studies.

The importance of being able to clearly differentiate between the boundary currents and the interior was shown in a detailed study of processes in the Labrador Sea by Straneo (2006). Considering two periods for which she had sufficient data, Straneo showed that lateral exchanges play a key role in balancing the surface fluxes. She also showed that interannual variations in the export of LSW is linked to changes in the interior boundary current density gradient, which governs the lateral exchange. Besides using higher-resolution oceanic fields, we also wanted to consider their variability, by being the first to include time-varying surface density fields (rather than using climatological surface properties) so that all of the variability is not driven purely by the surface fluxes, which are known to be closely correlated with the NAO (Hurrell et al. 2003). To provide a greater understanding of the variability, we provide detailed uncertainty estimates of LSW transformation/formation, as well as examining the role played by each of the components in the buoyancy flux. We also consider the sensitivity of LSW transformation/formation to several facets of recently observed Labrador Sea variability, such as the increased precipitation and long-term freshening. Finally, with the understanding that the density of LSW varies with time, we also provide formation estimates for several different density ranges.

Section 2 thus discusses the method that we use, as well as the data. Mean water mass transformations rates and their sensitivity are examined in section 3, while their long-term variability is dealt with in section 4. Finally, a summary and discussion is presented in section 5.

2. Methods and data

As this method has been presented in a number of papers previously (Speer and Tziperman 1992; Tziperman and Speer 1994; Speer et al. 1995), we shall only summarize it here. Following the above references, the instantaneous cross-isopycnal volume flux due to buoyancy forcing in the surface layer, $F(\rho')$, is given by

$$F(\rho') = \int_{\text{year}} dt \int_A dx\, dy \left[\frac{\alpha}{C_p} \mathcal{H}(x, y, t) - \rho \beta S(x, y, t) Q(x, y, t) \right] \delta[\rho(x, y, t) - \rho'], \quad (1)$$

where $\mathcal{H}(x, y, t)$ and $Q(x, y, t)$ are the surface fluxes of heat and freshwater, $\mathcal{A}$ is the area over which the calculation is performed; C_p is the specific heat capacity of water while α and β are the derivatives of density with respect to temperature and salinity respectively, $S(x, y, t)$ is the surface salinity, and $\rho(x, y, t)$ is the surface density. The delta function in the integral means that for any given surface density the surface buoyancy fluxes only produce transformations when the surface density is of that given value. Note that we define $\mathcal{F}$ in terms of buoyancy forcing, rather than in terms of the density flux, and thus negative $\mathcal{F}$ can be associated with a transformation of water to a given density.

In practice, the data fields used are not continuous, and a discrete formulation is used. This replaces the delta function with a boxcar function that is equal to one when the surface density is in the range $(\rho' - \frac{1}{2}\delta\rho, \rho' + \frac{1}{2}\delta\rho)$ and is zero otherwise. We use $\delta\rho = 0.05$ kg m^{-3} as a compromise between resolution and noise (Tziperman and Speer 1994). The area for which we perform the calculation over is 50°–64°N, 45°–60°W, while the time integration is done monthly. To provide an estimate of the uncertainty, we use a Monte Carlo simulation with 1000 draws. For each draw, we perturb the fluxes (heat and freshwater) and the surface density by drawing randomly from three different normal distributions, each one with a width (standard deviation) given by the spatial mean of the standard deviation of the corresponding field (34.9 W m^{-2}, 8 cm yr^{-1}, and 0.009 kg m^{-3}). These uncertainty estimates agree well with those used by Isachsen et al. (2007) in the Nordic seas.

We use surface fluxes of heat and freshwater from the NCEP–NCAR model reanalysis, described in Kistler et al. (2001). The NCEP–NCAR reanalysis is based on the 1995 version of the NCEP model and has a horizontal resolution of about 210 km, which is linearly interpolated to ⅓° to match the resolution of the ocean surface fields. We use the data for the period 1949–99 but focus on 1960–99, as the earlier fields are less reliable due to reductions in the amount and type of data available for assimilations (Kistler et al. 2001).

We use the daily fluxes and monthly average them as that is the temporal resolution of the ocean surface data we use. We examined directly using the daily fluxes with no monthly averaging and found no difference in our results, as the ocean is responding to the total buoyancy loss applied over each month. We note this would not hold if we were able to consider the more realistic situation of the ocean surface density varying over the course of the month in response to the surface fluxes. Isachsen et al. (2007) discuss the issue of daily versus monthly fluxes in more detail. They show that surface transformation rates estimated from monthly mean data match the large-scale diapcynal overturning circulation, at least in the Nordic seas, to lowest order even if other studies (Cerovecki and Marshall 2008; Tandon and Zhao 2004) suggest that using monthly instead of daily data will significantly overestimate the net transformation.

The NCEP–NCAR heat fluxes are known to have some issues in the Labrador Sea. Renfrew et al. (2002) showed that the NCEP–NCAR reanalysis data significantly overestimate the latent (by 27%) and sensible (by 51%) heat loss in the Labrador Sea. To examine the significance of these errors, we also recompute our transformation and formation rates using fluxes reduced by the size of the overestimates given by Renfrew et al. (2002), again using 1000 draws in the Monte Carlo simulation. Previous works (Josey and Marsh 2005; Myers et al. 2007a) suggest that there is not a significant discrepancy between temporal variability of precipitation estimates derived from NCEP–NCAR and the ECMWF reanalysis, as well as with a limited comparison of gauge data around the subpolar gyre.

The ocean data (temperature and salinity) used are based on a series of climatologies of the Labrador Sea produced using all available stations with both temperature and salinity measurements that were in the Fisheries and Oceans Canada hydrographic climate database (Gregory 2004) prior to 2000. Our "base" state is the monthly geopotential climatology of Kulan and Myers (2007, manuscript submitted to *Atmos.–Ocean*). We choose the geopotential climatology even though Kulan and Myers considered their isopycnal climatology better represented the large-scale water mass structure of the Labrador Sea because of issues with the interpolation of the shallowest isopycnal surface to the ocean's surface. Additionally, the data were mapped into overlapping 3-yr running mean triads, covering the period 1949–99 (Kulan 2007). Each triad was defined to include all data collected in a given year, as well as all available data in the preceding and following year. The triad data was binned into 2.5° (south of 55°N) or 5.0° boxes (north of 55°N) to provide a first guess for an objective analysis procedure that used three passes with decreasing correlation lengths of 600, 400, and 200 km, weighted by a severe topographic constraint to minimize mixing of waters across the shelf break. The use of larger correlation lengths than for the climatological analysis (Kulan and Myers 2007, manuscript submitted to *Atmos.–Ocean*) was to deal with issues of data scarcity in the central and northern parts of the domain in some years. The mapping was carried out in an isopycnal framework using 44 density layers and ⅓° spatial resolution.

We then computed the mean and anomalies for the temperature and salinity for each grid point over the period 1949–99. These anomalies were then added to the base monthly climatology for each year to give us monthly and interannually varying surface fields of temperature and salinity. We choose this approach as the triad fields were biased toward the summer when the majority of the observations were taken. Our assumption is that interannual variations in the hydrography are fairly independent of season (i.e., fresh years will be fresher than average in all seasons, e.g., during GSA events). Density was determined using the UNESCO formula (Fofonoff and Millard 1983). As with the surface fluxes, the triads from the earlier years have more issues than for the later years when more data exist.

We show the annual and winter, January–March (JFM), averages of the heat and freshwater fluxes expressed as buoyancy flux (Fig. 2), as well as the standard deviation for the winter fields (Fig. 3), over 1949–99. The main component of the buoyancy flux is due to the heat loss, which is focused over the north-central part of the domain, with an extension of the strong heat losses down the Labrador side of the basin in winter. Precipitation is generally largest in the coastal regions and the net buoyancy flux due to this term is generally smaller than from the heat fluxes (by one order of magnitude), although we note a nonzero buoyancy loss due to evaporation in the interior in winter. Both flux components exhibit strong variability in the northern Labrador Sea, decreasing toward the south (Fig. 3). But greater insight into the variability can be seen by comparing the fluxes between two pentads, one when the NAO was low (1963–67) and another when the NAO index was high and significant LSW formation occurred (1988–92) (Haine et al. 2008). Although the maximum value of the buoyancy loss has changed little between the pentads, the region of maximum loss has enlarged and shifted to the south during 1988–92. We note that this shift places it almost directly on top of the main site where LSW is believed to form (Clarke and Gascard 1983). A greater buoyancy loss also occurs over most of the south-central part of the basin in the high NAO pentad as well. There is also more variation between years in this later period (Fig. 4) in the northern part of the domain. Increased winter evaporation over the interior of the Labrador Sea is also seen in the pentad associated with a strong NAO (1988–92).

To consider the impact of any net supply of freshwater through the net advection of sea ice into the Labrador Sea on water mass transformation, we use the 1° monthly Northern Hemisphere dataset of Walsh (1978). We determine the month with the maximum ice concentration in each grid cell and extract the mean concentration for that month over the period 1950–99. We also extract the single maximum concentration in each grid cell over the entire 50-yr period to investigate the maximum possible impact of ice melt. We obtain thickness from a 13-yr simulation of an eddy-permitting simulation of the North Atlantic Ocean using the Nucleus for European Modelling of the Ocean (NEMO) model (Madec 2008), which includes a component based upon the Louvain-la-Neuve sea ice model (Fichefet and Morales Maqueda 1997). Where there is a mismatch between the model and the climatology concentration fields, we use a thickness of 10 cm. For simplicity, we assume that all of the ice forms and then melts within the given grid point and consider the associated freshwater flux as a buoyancy flux. Examining that flux (Fig. 2), we see that it is quite significant along the Labrador coast but does not play a significant role in the interior, which has little sea ice (and what exists is very thin). Whether a higher-resolution Labrador Sea ice climatology might produce a more significant impact is an open question since, at the very least, the presence of sea ice in the West Greenland Current is missing from the climatological analysis used. In any event, we use these results to justify not including the impact of the sea ice in any further calculations.

The maximum surface density (and its variability) is given in Fig. 5. Low densities are found in the boundary currents, while highest densities are found in a broad horseshoelike pattern around the northern part of the basin. Long-term mean density anomalies stay below 27.70 due to (i) inclusion of data from different years with significantly different conditions in the objective analysis and (ii) the lack of wintertime data, especially during the actual convective events, when the surface density reaches its maximum. Using data from a winter cruise in 1997, Pickart et al. (2002) showed that surface densities reached 27.78 kg m^{-3} in the western Labrador Sea. Additionally, since the method only considers the surface densities and surface fluxes, the impact of the entrainment of salty Irminger Water into LSW is not taken into account, which has been shown to be important by Straneo (2006). Variability is fairly consistent throughout the entire interior and, in fact, varies little over our entire study region (Fig. 5). We also note that the region where convection is known to occur (Clarke and Gascard 1983) is not a location of a maximum in the long-term mean surface density. Instead, years of strong convection are associated with a southward displacement of the maximum surface density into this area (as well as an increase in the actual maximum density).

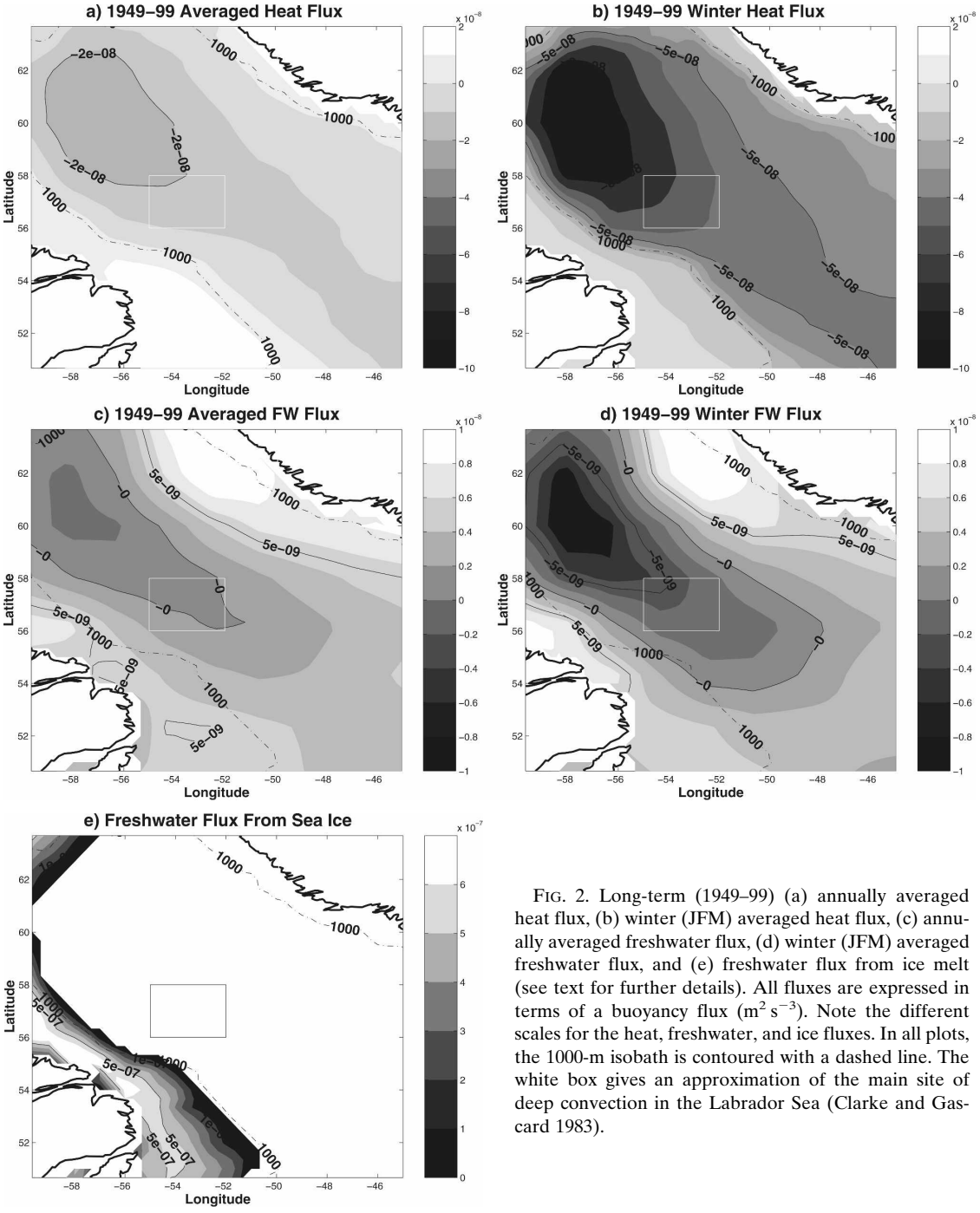

FIG. 2. Long-term (1949–99) (a) annually averaged heat flux, (b) winter (JFM) averaged heat flux, (c) annually averaged freshwater flux, (d) winter (JFM) averaged freshwater flux, and (e) freshwater flux from ice melt (see text for further details). All fluxes are expressed in terms of a buoyancy flux ($m^2\,s^{-3}$). Note the different scales for the heat, freshwater, and ice fluxes. In all plots, the 1000-m isobath is contoured with a dashed line. The white box gives an approximation of the main site of deep convection in the Labrador Sea (Clarke and Gascard 1983).

3. Mean water mass transformations

We first present the mean annual transformation rate (Fig. 6), with uncertainty. It is determined by computing the transformation rate for each density class each year and then averaging over a given time period. Very little transformation occurs at low densities (not shown) with weak peaks of 0.15 ± 0.06 Sv at $\sigma = 24.6$ kg m^{-3} and 0.15 ± 0.05 at $\sigma = 25.6$ kg m^{-3}. The peak at around $\sigma = 26.7$ kg m^{-3} of close to 1.1 ± 0.2 Sv is associated with the transformation of more dense water to lighter during the restratification process through heating by shortwave radiation and freshwater gain from the boundary currents/atmosphere in spring/summer.

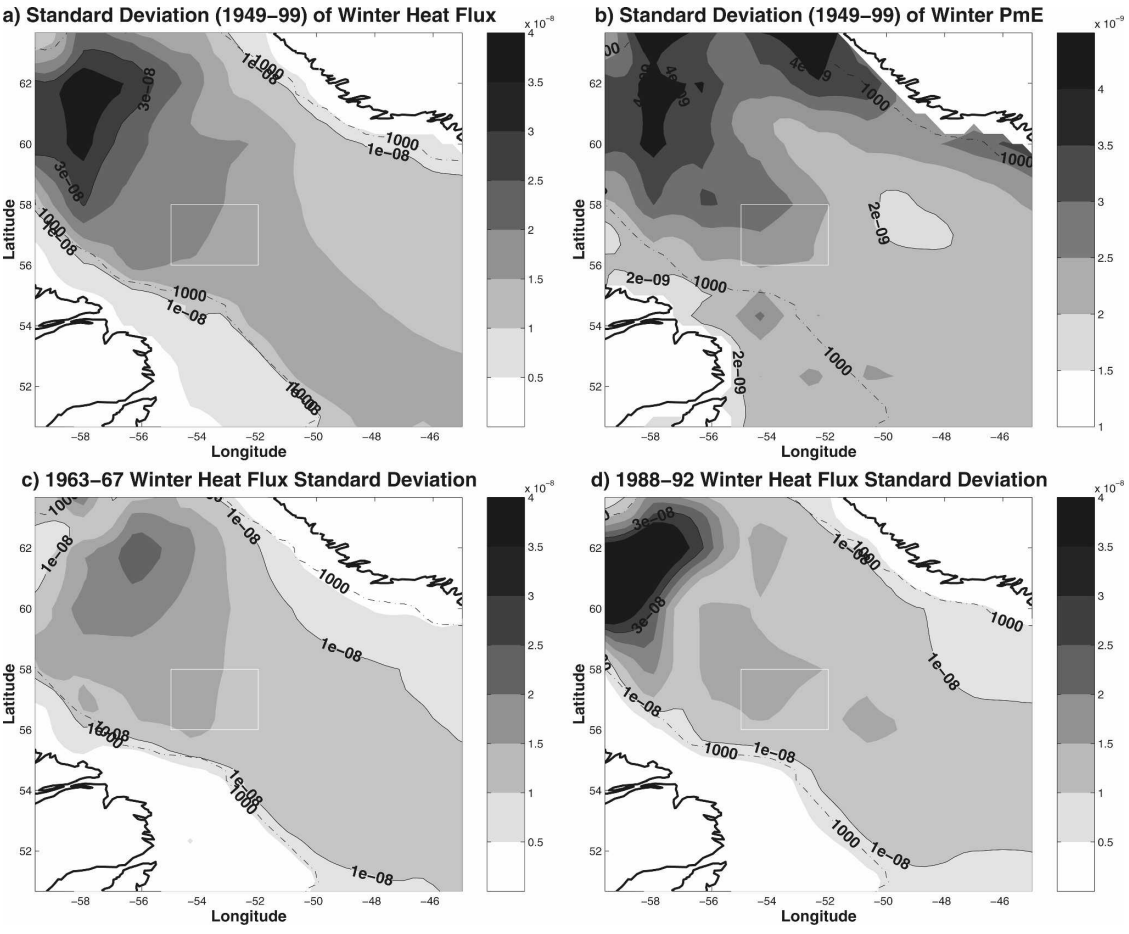

FIG. 3. Standard deviation (1949–99) of (a) winter (JFM) heat flux and (b) winter (JFM) freshwater flux, expressed as a buoyancy flux. Standard deviation of winter (JFM) heat fluxes for pentads (c) 1963–67 and (d) 1988–92. All fluxes are expressed in terms of a buoyancy flux ($m^2\ s^{-3}$). The white box gives an approximation of the main site of deep convection in the Labrador Sea (Clarke and Gascard 1983). Note that the scale for (b) differs by an order of magnitude.

Wintertime cooling leads to a mean long-term transformation rate of 3.9 ± 0.3 Sv of water to densities greater than $\sigma = 27.65$ kg m^{-3}. Our uncertainty estimates of 0.2–0.3 Sv from the Monte Carlo analysis are smaller than those of Isachsen et al. (2007). Besides being for a different region, this difference in error magnitude is probably because they randomly choose between two different surface flux climatologies in their analysis, which we suspect would lead to much greater variability in the heat flux forcing and thus transformation rate. All three components of the outgoing fluxes play a non-negligible role in the transformation process at greater densities, with the sensible and latent components the largest. The sensible heat flux is the largest contributor because of a region of very high buoyancy losses in the northwest corner of the basin where the sensible heat loss is up to 60% larger than the latent heat loss. Using reductions based upon Renfrew et al. (2002) for the latent and sensible heat fluxes, we find a mean transformation rate to densities greater than $\sigma = 27.65$ kg m^{-3} of 2.1 ± 0.2 Sv, which we can use as a lower bound on the transformation rate.

Our estimate of 3.9 ± 0.3 Sv is much larger than the 1.5 Sv estimated by Speer et al. (1995) but closer to the estimates of 2.7 Sv by Khatiwala et al. (2002) and 3.4 Sv by Marsh (2000). As Speer et al. (1995) used data from the 1980s and before, they could not include the intense convection periods of the late 1980s and early 1990s. Although the Marsh estimate is closer, we note that he found the mean year-round surface density maximum of $\sigma \geq 27.65$ kg m^{-3} extended widely into the Irminger Sea. We note also that the estimate of Marsh (2000) is based upon a shorter period that is mainly associated with high NAO index (Greatbatch 2000) and thus stronger convection (Curry and McCartney 2001). Meanwhile, our estimate over 1960–99 includes the period of the original GSA of the late 1960s that was associated with an extended period of weak LSW for-

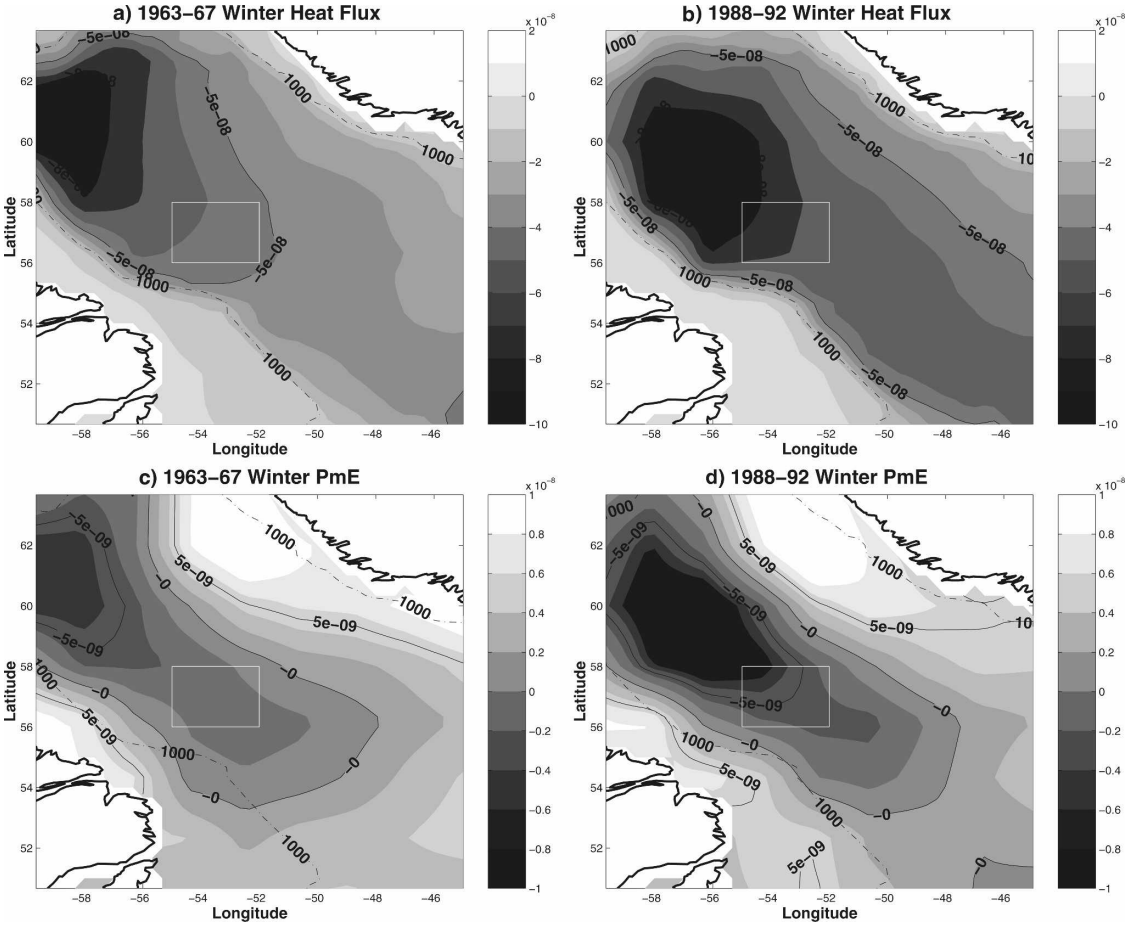

FIG. 4. Buoyancy flux associated with wintertime heat flux for the pentads (a) 1963–67 and (b) 1988–92. Buoyancy flux associated with wintertime freshwater flux for the pentads (c) 1963–67 and (d) 1988–92. All fluxes are expressed in terms of a buoyancy flux ($m^2\ s^{-3}$). The white box gives an approximation of the main site of deep convection in the Labrador Sea (Clarke and Gascard 1983).

mation (Dickson et al. 1988). One factor in our estimate being larger is the higher resolution of ocean surface data. If we degrade our fields to a resolution of 1° and repeat our analysis, our maximum transformation rate decreases to 3.5 Sv as the region with maximum density decreases. Beyond the direct resolution difference, the use of global climatologies leads to broad regions of low surface density throughout the western Labrador Sea, which probably explains the lower estimates found by Khatiwala et al. (2002) using the same fluxes.

Comparing with estimates from hydrographic sources, 3.9 ± 0.3 Sv falls well within the broad range discussed by Haine et al. (2008) and is not that much lower than Rhein et al.'s (2002) estimate of 4.4–5.6 Sv. However, this is only the formation rate of classical LSW, and Kieke et al. (2006) found that the formation of a lighter component of upper LSW was 3.2–3.3 Sv over 1970–97, for a combined LSW formation rate of 7.6–8.9 Sv. The above estimates may include formation outside of the Labrador Sea, which is not considered in this study. Kieke et al. (2006) suggest that, at least in the late 1990s, all of the upper LSW could not be formed in the Labrador Sea, while Pickart et al. (2003) and Falina et al. (2007) have discussed the potential for LSW formation in the Irminger Sea, potentially explaining part of the difference between our estimates and those of Kieke et al. (2006), although the difference may be also because of the difference in approaches used (water mass transformation versus tracers). If we include the years before 1960 (1949–59), we find a smaller formation rate of 3.2 ± 0.3 Sv. Further investigation suggests this is an artifact of the data in those early years since Curry et al. (1998) showed that thickness of LSW was much greater in the first half of the 1950s than in the second half, which points to convective renewal.

As was found by Speer and Tziperman (1992), basically all of the mean transformation is driven by the heat fluxes with the precipitation only weakly acting to

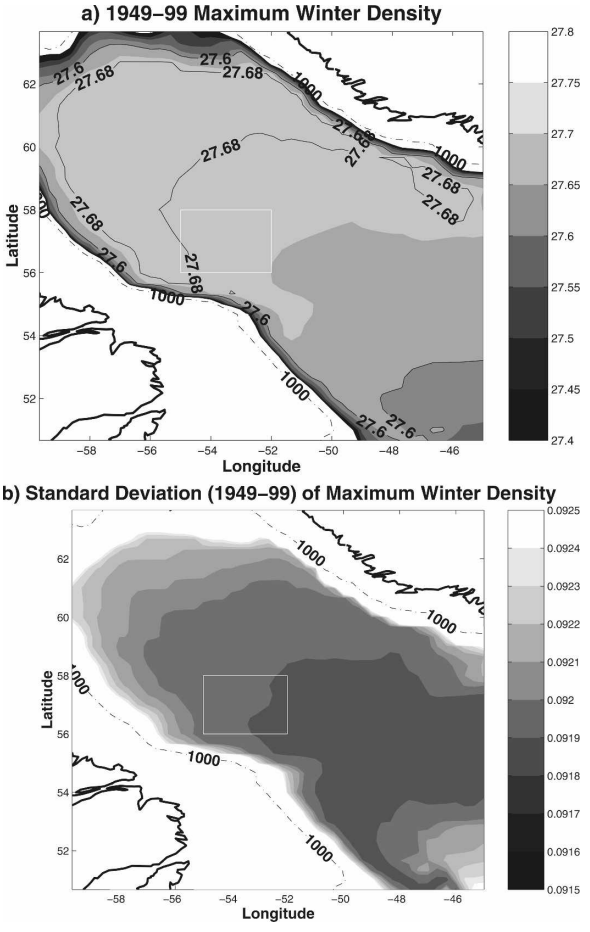

FIG. 5. (a) Mean (1949–99) annual maximum winter density anomaly and (b) standard deviation (1949–99) of maximum winter anomaly density. Units are kg m^{-3}. The white box gives an approximation of the main site of deep convection in the Labrador Sea (Clarke and Gascard 1983).

oppose formation of water at high densities. Despite this, we were still curious whether the long-term observed increases in precipitation might be impacting on LSW formation. Myers et al. (2007a) found that excess precipitation over the interior of the Labrador Sea had increased from 22 cm yr^{-1} for the period of 1960–74 to 31 cm yr^{-1} for 1975–2000. To examine any possible sensitivity to this increase, we take our net precipitation for each month and year and modify it (both positively and negatively) by 5, 10, or 25 cm yr^{-1} (Fig. 7a). This shows that these changes in atmospheric forcing have had little impact on the transformation process in the Labrador Sea. With an increase in net precipitation of 10 cm yr^{-1}, the amount closest to the observed increase, we find a decrease in the maximum transformation rate of only 0.1 Sv.

As seen in our buoyancy fluxes plots (Fig. 4), there can be large variations in wintertime heat loss over the Labrador Sea, with average heat losses varying by up to 100 W m^{-2} between high and low NAO years (Pickart et al. 2002). We thus consider the case when our heat fluxes are modified for each month and year (both positively and negatively) by 10, 25, and 100 W m^{-2} (Fig. 7b). As might be expected, this shows a much larger sensitivity with variations in the maximum transformation flux of 2.6 Sv between extreme and normal years.

As well as the surface fluxes, the surface water properties will change with time, and, because of the way that the water mass diagnostic approach is formulated, one must also consider changes in surface temperature and salinity and thus density. We first vary the surface water temperatures (both positively and negatively) by 0.5° and 1.0°C (Fig. 8a). We see two interesting processes occurring here. As surface temperatures are increased, transformation rate maxima and minima generally shift to lower density. Although this might be expected, there is also a general decrease in the transformation rate at highest density as temperatures are decreased, while the transformation rate minimum at high densities becomes more negative with increasing temperatures. This later effect may arise because, as the maximum density decreases, the peak in the transformation shifts to less dense water classes, which are transformed at a higher rate as the surface area with those densities increases. The seemingly contradictory decrease in transformation with cooler surface temperatures is a function of how changes in temperature affect density. As the relationship between temperature and density is nonlinear, a constant decrease in temperature will not always lead to the same increase in density. Thus all of the water at the maximum density may not end up in the bin associated with the new maximum in density.

Since the effects of salinity on density are more linear than temperature, we might expect variability in surface salinity to have a more straightforward effect on transformation. Thus we allow the surface salinity to vary (both positively and negatively) by 0.02, 0.05, 0.1, and 0.2 (Figs. 8b,c). Here we see that changes in salinity lead to an increase or decrease in the densities of the transformed waters in the Labrador Sea, but no appreciable change in the volume of transformation. So, it is the pairs of temperature and salinity that determine the surface density and hence the type/class of LSW formed, while it is the heat fluxes that determine the transformation rate.

4. Interannual variability

To look at interannual variability, we use formation rather than transformation. This is done to clearly high-

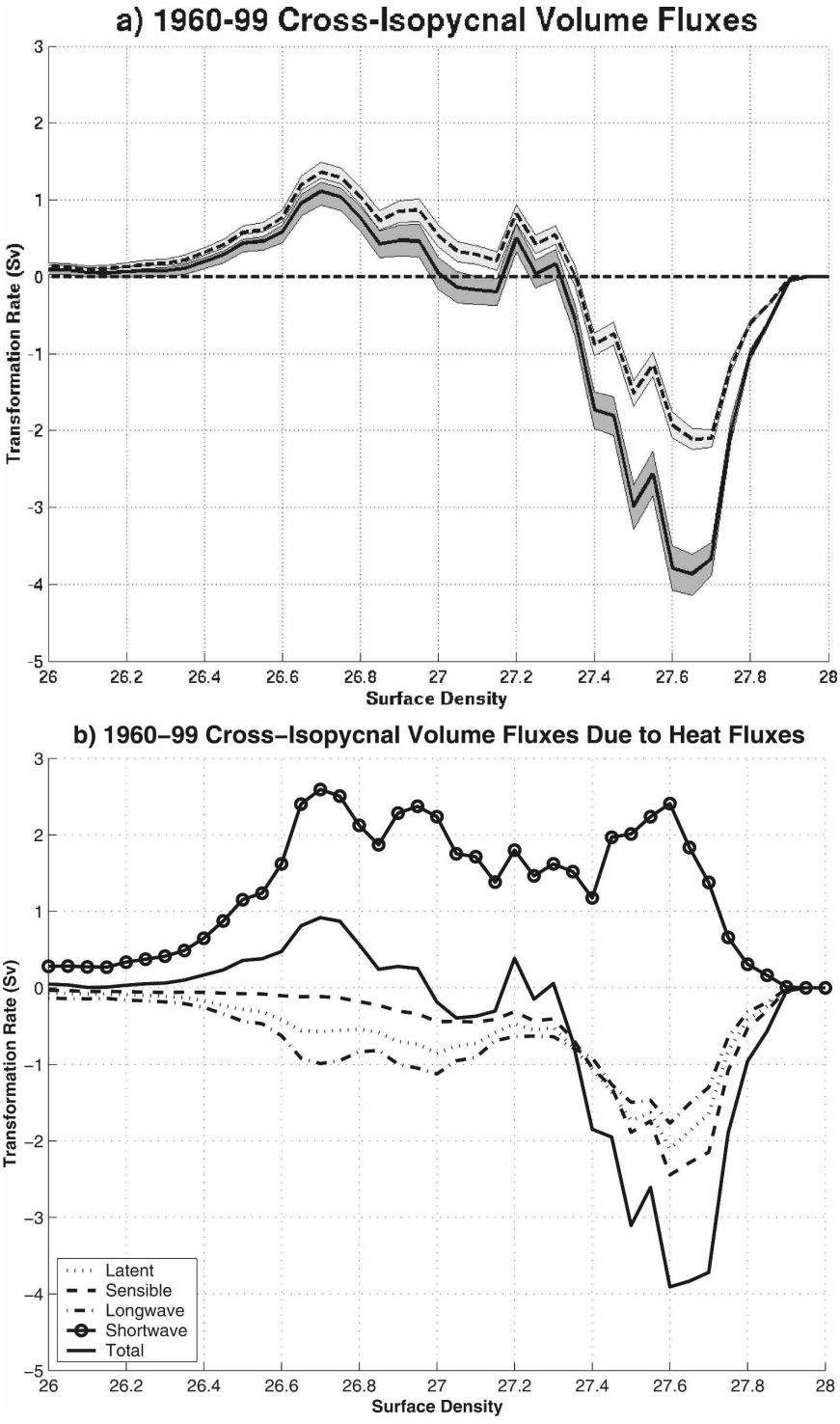

FIG. 6. Cross-isopycnal volume fluxes as a function of surface density, computed for 1960–99: (a) using both components of the buoyancy flux, with uncertainty, using the full NCEP fluxes (solid line, dark gray shading) and the NCEP latent and sensible heat fluxes reduced based upon Renfrew et al. (2002) (dashed line and light gray shading); (b) cross-isopycnal mass fluxes for each of the heat flux components separately (using the full NCEP fluxes). Positive values represent an input of buoyancy, while negative values point to a removal of buoyancy.

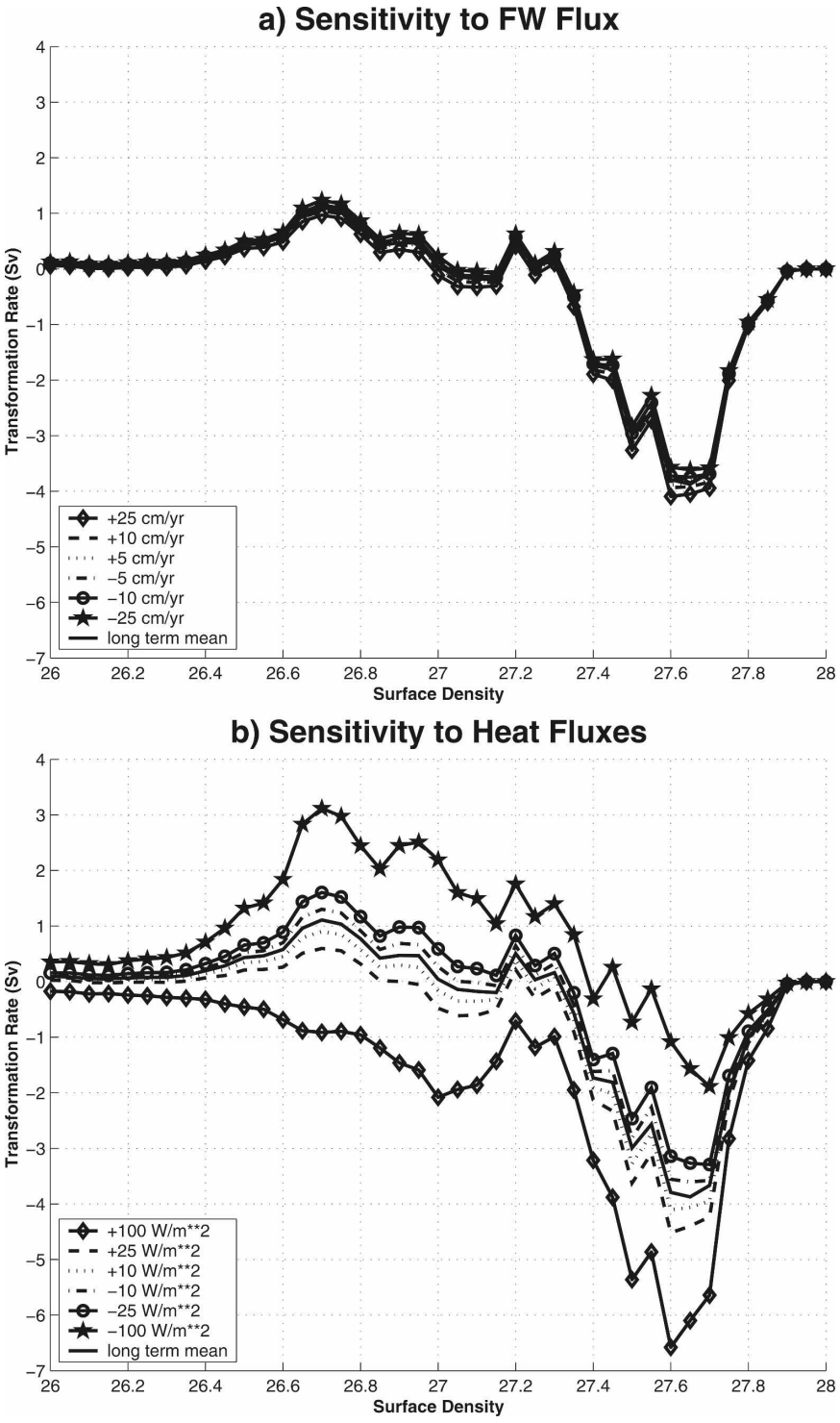

FIG. 7. The sensitivity of the cross-isopycnal volume fluxes (for 1960–99) to variability in the (a) freshwater component of the buoyancy fluxes and (b) the heat component of the buoyancy fluxes.

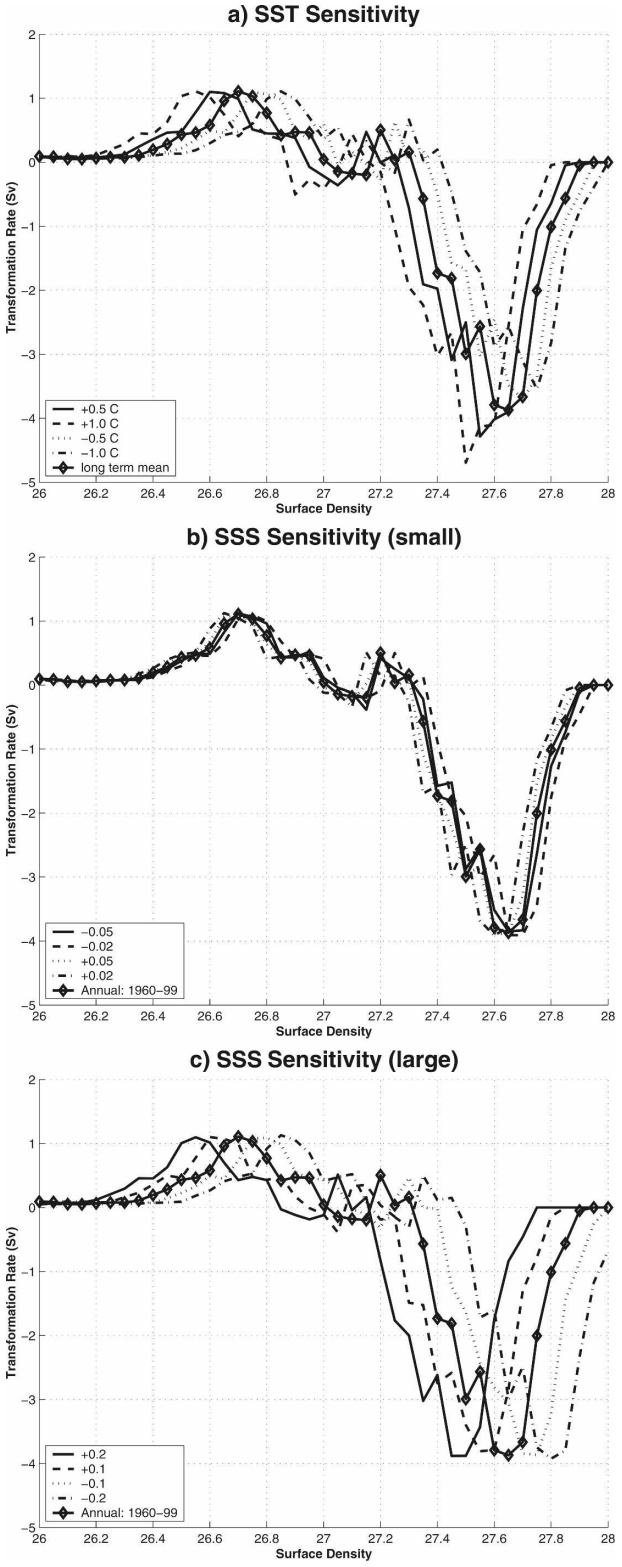

FIG. 8. The sensitivity of the cross-isopycnal volume fluxes (for 1960–99) to variability in the (a) surface temperature and (b), (c) surface salinity. Note that (b) and (c) are otherwise the same except for different magnitudes of salinity change.

light the year to year variability in formation and different densities, considering the significant variability in both surface water properties and forcing with time and the sensitivity of variability to temperature and salinity discussed above. The formation is the rate of change of transformation per unit mass,

$$M(\rho) = \frac{-dF}{d\rho},$$

and was first examined by Speer and Tziperman (1992).

We thus calculate the formation rate, with error bars, for three density ranges for the years 1960–99 (Fig. 9). For two ranges, we focus on LSW with densities of $\sigma = 27.675 - 27.725$ kg m^{-3} and $\sigma > 27.725$ kg m^{-3}. Although the densities ranges are not exactly consistent with those for upper and classical LSW, we may be able to consider the two time series as roughly analogous to those two types of LSW. Additionally, we consider a broad range of densities, $\sigma > 27.625$ kg m^{-3}, which includes subpolar mode water as well as LSW but is maybe indicative of all the dense water products that are being produced in the Labrador Sea.

We find mean formation rates of 1.7 ± 0.3 Sv for $\sigma = 27.675 - 27.725$ kg m^{-3} and 2.0 ± 0.3 Sv for $\sigma > 27.725$ kg m^{-3} using unmodified NCEP fluxes and 0.9 ± 0.2 Sv and 1.2 ± 0.2 Sv, respectively, correcting the fluxes as per Renfrew et al. (2002). The smaller uncertainty associated with the corrected fluxes is a function of the reduced fluxes having smaller means, and thus a narrower distribution in the Monte Carlo analysis. Our combined category, $\sigma > 27.625$ kg m^{-3}, has a mean consistent with the long-term transformation rate, 3.9 ± 0.3 Sv (2.1 ± 0.2 Sv with the reduced fluxes).

However, more than any interannual or interdecadal variability, the most striking feature is the off/on structure of LSW formation in our time series. We see that the years with actual formation are generally associated with much more formation than the long-term means, which are then averaged over years of strong water formation and no water formation. Uncertainties reach 0.7–1.8 Sv in years of strong water formation but are always small compared to the actual formation in a given year, suggesting the variability represented is real.

Five strong formations events are observed over the 40 yr (Fig. 9c). The events in the 1970s and early 1980s were quite short in duration (1–2 yr), while the other events were each at least half a decade in length. This would be consistent with the idea of Yashayaev et al. (2007) that LSW can be defined in terms of classes associated with a common development history over a

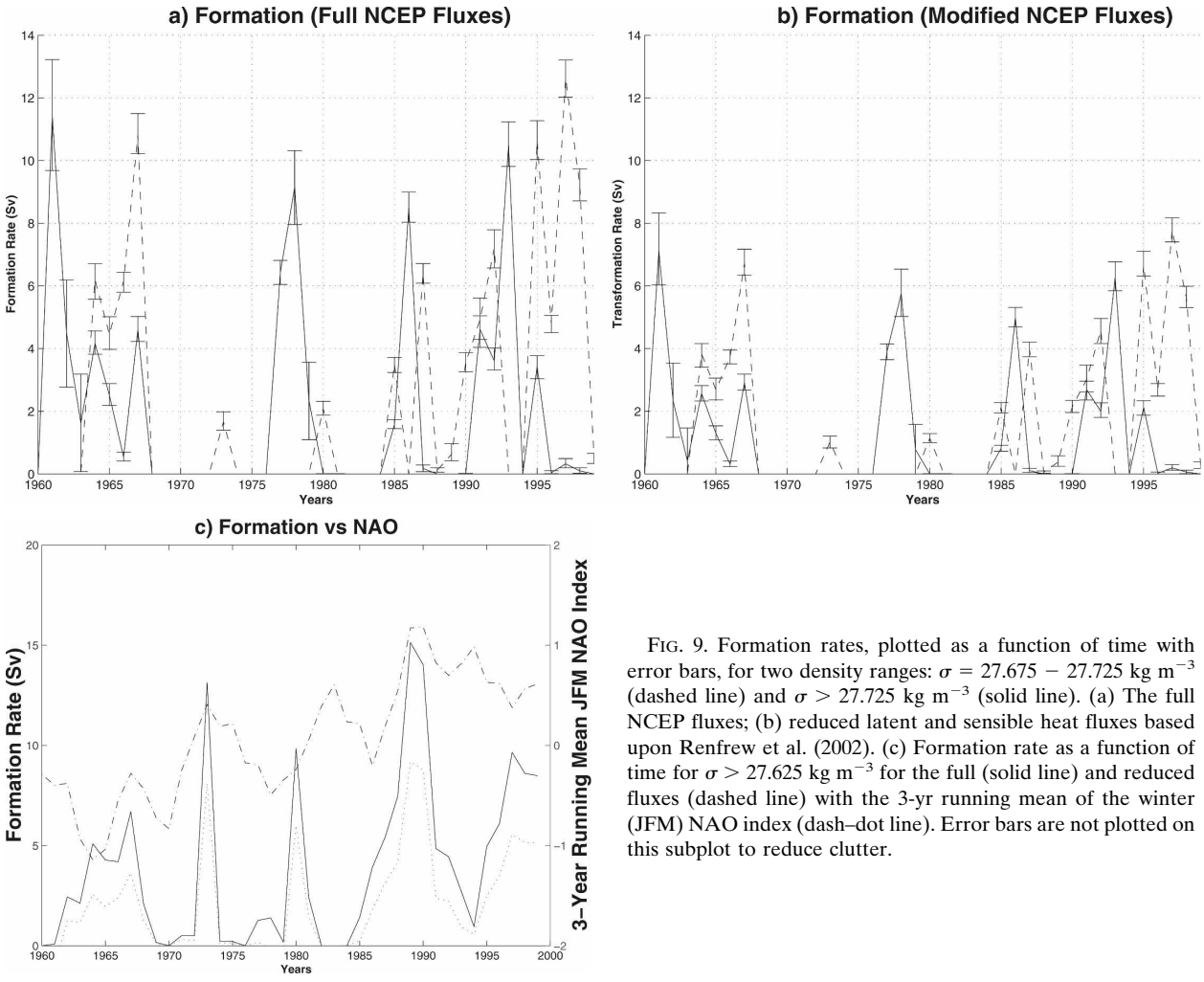

FIG. 9. Formation rates, plotted as a function of time with error bars, for two density ranges: $\sigma = 27.675 - 27.725$ kg m^{-3} (dashed line) and $\sigma > 27.725$ kg m^{-3} (solid line). (a) The full NCEP fluxes; (b) reduced latent and sensible heat fluxes based upon Renfrew et al. (2002). (c) Formation rate as a function of time for $\sigma > 27.625$ kg m^{-3} for the full (solid line) and reduced fluxes (dashed line) with the 3-yr running mean of the winter (JFM) NAO index (dash–dot line). Error bars are not plotted on this subplot to reduce clutter.

limited number of years. Looking at the most dense class, four strong formation events for densities greater than $\sigma = 27.725$ kg m^{-3} are observed, each lasting 2 to 4 yr, except during the 1960s when there were seven consecutive years with formation. The maximum formation rate for these events is remarkably consistent for all four episodes (8.5–11.4 or 5.0–7.1 Sv, depending on the version of the fluxes used). In general, if formation occurs for densities of $\sigma > 27.725$ kg m^{-3}, it does not also occur at lighter densities ($\sigma = 27.675 - 27.725$ kg m^{-3}), although in a few years (1964, 1967, 1991, 1992, and 1995) formation of greater than 2 Sv occurs for both density ranges. During these years, the formation at the lighter densities occurs in the southern half of the Labrador Sea, south of the region of maximum surface density (Fig. 5). Other than a period of strong formation during the second half of the 1960s, formation for densities $\sigma = 27.675 - 27.725$ kg m^{-3} has tended to increase with time, especially during the later half of the 1990s. In between are years of little or no formation, associated with low surface densities. These include the periods associated with the first two GSAs (1970–71 and 1982–84). The impact of the low salinity water of the first GSA may be overemphasized in our analysis. Yashayaev (2007) and Clarke and Gascard (1983) have discussed convection events that occurred during the 1970s, whereby the low salinity water of the GSA was flushed down into the interior of the Labrador Sea. If we look at those years in more detail, we do find strong formation of 12 Sv in 1973, but only if we look at a more broad range of densities ($\sigma >$ 27.625 kg m^{-3}).

The variability otherwise compares well with other estimates of LSW formation in both phase and amplitude (e.g., Haine et al. 2008). Considering our two density ranges that may be considered LSW, we find a maximum formation rate of 9.5–10.8 ± 0.7–1.1 Sv for 1991–93 (5.7–6.6 ± 0.5–0.7 Sv using the modified

fluxes), consistent with the estimate of Marsh (2000) of ~10 Sv in 1990. Lazier et al. (2002) point out that intense convection occurred during 1990–93, while Rhein et al. (2002) show the LSW formation reached a maximum of 8.1–10.8 Sv between 1988 and 1994. Yashayaev et al. (2007) also defined a 1988–94 LSW class. We see fairly high formation rates in our plots, although our averages for 1988–94 are 2.3 ± 0.3 and 2.7 ± 0.2 Sv, respectively, for a total formation rate of 5.0 ± 0.5 Sv during this period (1.5 ± 0.2, 1.6 ± 0.1, and 3.1 ± 0.3 Sv, respectively, using the modified fluxes). We also see a fall off in formation for densities of $\sigma > 27.725$ kg m^{-3} in the later part of the 1990s, as found by Rhein et al. (2002). During this period, our formation in the lighter density range, possible upper LSW, is 9.3 ± 0.5 Sv over 1995–98, 7.5 ± 0.4 Sv over 1995–99, and 4.8 ± 0.4 Sv over 1998–99, both of which compare favorably with the estimate of Kieke et al. (2006) who found a formation rate of 6.9–9.2 in 1998–99. Even using the reduced fluxes, estimates of 6.3 ± 0.5 Sv for 1995–98 and 5.1 ± 0.5 Sv for 1995–99 do not compare unfavorably.

Looking at what is driving the variability, we examine links between our formation rate estimates and the NAO. To represent the NAO, we use an index produced by the NOAA/National Weather Service Climate Prediction Center (CPC). The index is obtained from a method described by Barnston and Livezey (1987) consisting of a rotated principal component analysis of observed 700-mb height anomalies. Surprisingly we find little link between the NAO and our time series of formation rate in our two LSW classes (correlation coefficient 0.12 and 0.04, neither of which are significant). Instead, the NAO is linked (correlation coefficient of 0.45, significant at the 99% level) with the overall formation rate for $\sigma > 27.625$ kg m^{-3}. In Fig. 9c we see that, except for during the early 1980s, each peak in the NAO index is linked with a peak in water formation rate. The lack of a water formation peak during the early 1980s when the NAO was strong is because of the input of low salinity water associated with the second GSA (Belkin et al. 1998). This confirms other studies (e.g., Haine et al. 2008) that showed that the NAO strength governs the formation rate. That we need to consider densities as low as $\sigma = 27.625$ kg m^{-3} to see this correlation is probably a function of two factors. One is almost certainly data related, with the lack of winter data biasing our surface densities to lower values. Additionally, it suggests that since the NAO changes the heat fluxes over much of the Labrador Sea, it is the entirety of water formation (rather than just LSW formation) that is being modulated by this forcing.

Additionally, Yashayaev et al.'s (2007) idea that Labrador Sea Water formation can be broken down into classes with a common formation history over a number of years is supported by this analysis. We find five classes of water formation in the Labrador Sea: 1962–68, 1971–74, 1977–81, 1986–92, and 1995–99. The period (3–5 yr) between the events is consistent with estimates of the flushing time scale of the Labrador Sea (Lazier et al. 2002), suggesting that eroding the stratification from the previous event may be necessary before the next event can occur. Although three of the events include formation of LSW in our most dense category, two (the early 1970s and the late 1990s) only involve formation in the lighter density categories. Since during both of these events the NAO is reasonably high (even if it is not approaching a maximum during the late 1990s), this suggests that, while the NAO may play a role in governing the formation rate, other factors, such as freshwater input, govern the class of LSW produced. The early 1970s event is associated with the flushing down of the freshwater associated with the first GSA (Houghton and Visbeck 2002), while the second occurred during a period when the long-term freshening of the Labrador Sea had reached a maximum (Yashayaev 2007). Since both salinity and temperature of the Labrador Sea have started to increase again over the last few years (Yashayaev 2007), possibly associated with an increase in the input of Irminger Water (Myers et al. 2007b), the question of whether we can expect future convection events to include LSW formation in the denser categories is open.

5. Summary and discussion

Objectively analyzed surface hydrographic fields and NCEP–NCAR reanalysis fluxes are used to estimate water mass transformation and formation rates in the Labrador Sea, focusing on LSW. We estimate a mean long-term transformation of between 2.1 ± 0.2 and 3.9 ± 0.3 Sv over the years 1960–99 to water with densities greater than $\sigma = 27.65$ kg m^{-3}, depending on whether we correct the latent and sensible heat fluxes based upon the work of Renfrew et al. (2002) or not. This suggests the importance of further work to improve measurements and bulk formula to give improved flux estimates over the Labrador Sea. We also show that these estimates are sensitive to the resolution of the ocean data used (degrading the resolution reduces the estimate by approximately 9%).

Breaking this down further, we find mean long-term formation rates of between 0.9 ± 0.2 and 1.7 ± 0.3 Sv for $\sigma = 27.675 - 27.725$ kg m^{-3} and 1.2 ± 0.2 and 2.0 ± 0.3 Sv for $\sigma > 27.725$ kg m^{-3}. There is tremen-

dous variability associated with these formation rates with years of strong water formation (5.7–6.6 ± 0.5–0.7 or 9.5–10.8 ± 0.7–1.1 Sv) mixed with years of little or no formation in the given density range. We also find a shift from strong convection in the denser of our two ranges during the early 1990s to convection in the less dense range during the later part of the 1990s, consistent with the observed shift from the formation of classical to upper LSW (Kieke et al. 2006). These values fit into the range suggested for LSW formation from a number of observational studies. Additionally, the strong convection of the early 1990s seems to be associated with a shift of the center of buoyancy loss southward to the main site of deep-water formation combined with the increase in overall buoyancy loss due to the NAO being in the high phase.

As known from previous studies (Tziperman and Speer 1994), basically all of the mean transformation is driven by surface heat fluxes. The observed long-term increase in net precipitation over the Labrador Sea does not seem to have had any significant effect on LSW, only reducing the LSW transformation rate by 0.1 Sv. The impact of sea ice melt in the interior of the Labrador Sea seems also to be negligible. However, the calculated transformation rates are sensitive to the surface water properties. A reduction in surface salinity leads to formation occurring at a reduced density, but with little change in the amount of water transformed. A decrease in surface temperature leads to a shift in the transformation rate maxima and minima to higher densities, as well as a general decrease in the transformation rate at highest densities. Our sensitivity analysis also suggests that changes in the heat fluxes can significantly impact the volume of water transformed but have little direct impact on the density of the transformed water mass. Although it is the heat fluxes that increase the surface density through fall and winter and our analysis is biased in that we use fixed surface water properties that cannot be changed by the fluxes, we do not think such a statement is unreasonable. The maximum density in the surface mixed layer is as much a function of oceanic advection and stratification as the air–sea fluxes, with increased surface heat loss leading at some point in time to mixed layer deepening rather than further increases in surface density. We also note that our analysis completely misses the impact of the entrainment of salty Irminger Water from below, which has been shown to be important (Straneo 2006).

Thus, as is widely accepted, variability in the amount of LSW formed is strongly linked to variability in the surface heat fluxes, which are strongly linked to atmospheric variability, such as the NAO (Curry and McCartney 2001). However, how the long-term freshening of the subpolar gyre is going to influence water mass formation in the Labrador Sea is by reducing the density of the convective products. We thus wonder if the recent shift from classical LSW formation to upper LSW is a sign of this freshening. As discussed by Kieke et al. (2006), in 1998–99, strong upper LSW formation was almost compensated for by a lack of classical LSW formation. Additionally, Kieke et al.'s (2006) time series of layer thicknesses for LSW suggests that the total thickness of both LSW water masses remains relatively constant and just the relative importance of each varies with time. Kieke et al. (2006) noted reduced upper LSW formation in 2000–01, but this may be just due to weaker air–sea fluxes that year. If the Labrador Sea continues to freshen, then we wonder if the lighter convective products will continue to dominate in the Labrador Sea, although the amount of these products formed will continue to vary with the surface fluxes. However, we note that Yashayaev (2007) reported an increase in salinity over the top 2000 m over the past decade in the Labrador Sea. Additionally, one could speculate that, if the general freshening of the subpolar gyre continued, a decrease in the densities of deeper classes of subpolar mode water formed in the eastern parts of the gyre would follow. However, such mode waters are also sensitive to other processes, and Hátún et al. (2005) have discussed circulation changes in the eastern part of the gyre that have led to record high salinities at the entrance to the Nordic seas. In fact, these changes were probably the trigger for the increased salinity seen by Yashayaev (2007) in the Labrador Sea.

If the climate continues to warm, as most studies presently predict (Watson et al. 2001), and more freshwater is provided to the North Atlantic from the Arctic, Greenland, and/or an enhanced hydrological cycle, this will lead to a decrease in the density of the convective products being formed (although the question of how this freshwater gets from the coastal region and boundary currents into the convective gyres must also be considered). This change in density may potentially be without a significant change in the amounts of those products ventilated. Many studies regarding the impact of freshwater link increased provision of freshwater to the convective regions of the North Atlantic to a weakening or collapse of the global overturning circulation (e.g., Vellinga and Wood 2002; Stouffer et al. 2007). But, if the primary impact of decreased surface salinities (and thus density) is to reduce the density of the water being formed, rather than the amount, the long-term behavior may be more complicated. Unless the salinity drops so drastically that no ventilation of the intermediate layers occurs (such as during the GSA

events), some sort of convective product will always be produced in the northern North Atlantic and then exported southward in the lower limb of the overturning circulation.

Additionally as a caveat to this study, we must remember that variability of the surface fluxes is not the only mechanism that influences LSW formation. Lazier et al. (2002) discuss that the Labrador Sea has a memory of previous convection events. In addition, winter stratification as well as the advection of warm and saline anomalies of Irminger Water from the West Greenland Current will impact LSW formation.

Acknowledgments. This work was funded by NSERC and CFCAS grants (the latter through the Canadian CLIVAR network). Chris Donnelly was also a recipient of an NSERC USRA during the time he worked on this project. We thank Tom Haine, Igor Yashayaev, and two anonymous reviewers for many useful comments that significantly improved the manuscript and Nilgun Kulan for development of the triad dataset used. NCEP reanalysis data provided by the NOAA/OAR/ESRL PSD, Boulder, Colorado, from their Web site at http://www.cdc.noaa.gov/.

REFERENCES

Barnston, A. G., and R. E. Livezey, 1987: Classification, seasonality and persistence of low-frequency atmospheric circulation patterns. *Mon. Wea. Rev.,* **115,** 1083–1126.

Cerovecki, I., and J. Marshall, 2008: Eddy modulation of air–sea interaction and convection. *J. Phys. Oceanogr.,* **38,** 65–83.

Clarke, R. A., and J.-C. Gascard, 1983: The formation of Labrador Sea Water. Part I: Large-scale processes. *J. Phys. Oceanogr.,* **13,** 1764–1778.

Curry, R. G., and M. S. McCartney, 2001: Ocean gyre circulation changes associated with the North Atlantic Oscillation. *J. Phys. Oceanogr.,* **31,** 3374–3400.

——, and C. Mauritzen, 2005: Dilution of the northern North Atlantic Ocean in recent decades. *Science,* **308,** 1772–1774.

——, M. S. McCartney, and T. M. Joyce, 1998: Oceanic transport of subpolar climate signals to mid-depth subtropical waters. *Nature,* **391,** 575–577.

——, R. R. Dickson, and I. Yashayaev, 2003: A change in the freshwater balance of the Atlantic Ocean over the past four decades. *Nature,* **426,** 826–829.

da Silva, A. M., C. C. Young, and S. Levitus, 1994: *Algorithms and Procedures.* Vol. 1, *Atlas of Surface Marine Data 1994,* NOAA Atlas NESDIS 6, 83 pp.

Déry, S. J., M. Stieglitz, E. C. McKenna, and E. F. Wood, 2005: Characteristics and trends of river discharge into Hudson, James, and Ungava Bays, 1964–2000. *J. Climate,* **18,** 2540–2557.

Dickson, R. R., J. Meincke, S.-A. Malmberg, and A. J. Lee, 1988: "The Great Salinity Anomaly" in the northern North Atlantic 1968–1982. *Prog. Oceanogr.,* **20,** 103–151.

——, J. Lazier, J. Meincke, P. Rhines, and J. Swift, 1996: Long-term coordinated changes in the convective activity of the North Atlantic. *Prog. Oceanogr.,* **38,** 241–295.

——, I. Yashayaev, J. Meincke, B. Turrell, S. Dye, and J. Holfort, 2002: Rapid freshening of the deep North Atlantic Ocean over the past four decades. *Nature,* **416,** 832–837.

Falina, A., A. Sarafanov, and A. Sokov, 2007: Variability and renewal of Labrador Sea Water in the Irminger Basin in 1991–2004. *J. Geophys. Res.,* **112,** C01006, doi:10.1029/2005JC003348.

Fichefet, T., and M. A. Morales Maqueda, 1997: Sensitivity of a global sea ice model to the treatment of ice thermodynamics and dynamics. *J. Geophys. Res.,* **102,** 12 609–12 646.

Fofonoff, N. P., and R. C. Millard Jr., 1983: Algorithms for computation of fundamental properties of seawater. UNESCO Tech. Papers in Marine Science 44, 53 pp.

Greatbatch, R. J., 2000: The North Atlantic Oscillation. *Stochastic Environ. Res. Risk Assess.,* **14,** 213–242.

Gregory, D. N., 2004: Climate: A database of temperature and salinity observations for the northwest Atlantic. Canadian Science Advisory Secretariat Research Doc. 2004/075, 10 pp.

Haine, T. W. N., and Coauthors, 2008: North Atlantic deep water transformation in the Labrador Sea, recirculation through the subpolar gyre, and discharge to the Subtropics. *The ASOF Science Book,* R. R. Dickson, J. Meincke, and P. Rhines, Eds., Springer, in press.

Hátún, H., A. B. Sandø, H. Drange, B. Hansen, and H. Valdimarsson, 2005: Influence of the Atlantic subpolar gyre on the thermohaline circulation. *Science,* **309,** 1841–1844.

Houghton, R. W., and M. H. Visbeck, 2002: Quasi-decadal salinity fluctuations in the Labrador Sea. *J. Phys. Oceanogr.,* **32,** 687–701.

Hurrell, J. W., Y. Kushnir, G. Ottersen, and M. H. Visbeck, Eds., 2003: *The North Atlantic Oscillation: Climate Significance and Environmental Impact. Geophys. Monogr.,* Vol. 134, Amer. Geophys. Union, 279 pp.

Isachsen, P. E., C. Mauritzen, and H. Svendsen, 2007: Dense water formation in the Nordic Seas diagnosed from sea surface buoyancy fluxes. *Deep-Sea Res. I,* **54,** 22–41.

Josey, S. A., and R. Marsh, 2005: Surface freshwater flux variability and recent freshening of the North Atlantic in the eastern subpolar gyre. *J. Geophys. Res.,* **110,** C05008, doi:10.1029/2004JC002521.

Khatiwala, S., P. Schlosser, and M. H. Visbeck, 2002: Rates and mechanisms of water mass transformation in the Labrador Sea as inferred from tracer observations. *J. Phys. Oceanogr.,* **32,** 666–686.

Kieke, D., M. Rhein, L. Stramma, W. M. Smethie, D. A. LeBel, and W. Zenk, 2006: Changes in the CFC inventories and formation rates of upper Labrador Sea Water, 1997–2001. *J. Phys. Oceanogr.,* **36,** 64–86.

Kistler, R., and Coauthors, 2001: The NCEP–NCAR 50-Year Reanalysis: Monthly means CD-ROM and documentation. *Bull. Amer. Meteor. Soc.,* **82,** 247–267.

Kulan, N., 2007: A diagnostic study of the Labrador Sea circulation based on climatological data analysis, and an insight into the freshwater source variability. Ph.D. thesis, University of Alberta, 233 pp.

Lab Sea Group, 1998: The Labrador Sea deep convection experiment. *Bull. Amer. Meteor. Soc.,* **79,** 2033–2058.

Lascaratos, A., 1993: Estimation of deep and intermediate water mass formation rates in the Mediterranean Sea. *Deep-Sea Res.,* **40,** 1327–1332.

Lazier, J., R. Hendry, A. Clarke, I. Yashayaev, and P. Rhines,

2002: Convection and restratification in the Labrador Sea, 1990–2000. *Deep-Sea Res.,* **49,** 1819–1835.

Levitus, S., and T. P. Boyer, 1994: *Temperature.* Vol. 4, *World Ocean Atlas 1994,* NOAA Atlas NESDIS 4, 117 pp.

——, R. Burgett, and T. P. Boyer, 1994: *Salinity.* Vol. 3, *World Ocean Atlas 1994,* NOAA Atlas NESDIS 3, 99 pp.

Madec, G., 2008: NEMO reference manual, ocean dynamics component: NEMO-OPA preliminary version. Note du Pole de modelisation, Institut Pierre-Simon Laplace, No. 27.

Marsh, R., 2000: Recent variability of the North Atlantic thermohaline circulation inferred from surface heat and freshwater fluxes. *J. Climate,* **13,** 3239–3260.

Myers, P. G., S. A. Josey, B. Wheler, and N. Kulan, 2007a: Interdecadal variability in Labrador Sea precipitation minus evaporation and salinity. *Prog. Oceanogr.,* **73,** 341–357.

——, N. Kulan, and M. H. Ribergaard, 2007b: Irminger Water variability in the West Greenland Current. *Geophys. Res. Lett.,* **34,** L17601, doi:10.1029/2007GL030419.

Pickart, R. S., W. M. Smethie Jr., J. R. N. Lazier, E. P. Jones, and W. J. Jenkins, 1996: Eddies of newly formed upper Labrador Sea water. *J. Geophys. Res.,* **101,** 20 711–20 726.

——, D. J. Torres, and R. A. Clarke, 2002: Hydrography of the Labrador Sea during active convection. *J. Phys. Oceanogr.,* **32,** 428–457.

——, M. A. Spall, M. H. Ribergaard, G. W. K. Moore, and R. F. Milliff, 2003: Deep convection in the Irminger Sea forced by the Greenland tip jet. *Nature,* **424,** 152–156.

Renfrew, I. A., G. W. K. Moore, P. S. Guest, and K. Bumke, 2002: A comparison of surface layer and surface turbulent flux observations over the Labrador Sea with ECMWF analyses and NCEP reanalyses. *J. Phys. Oceanogr.,* **32,** 383–400.

Rhein, M., and Coauthors, 2002: Labrador Sea Water: Pathways, CFC inventory, and formation rates. *J. Phys. Oceanogr.,* **32,** 648–665.

Speer, K. G., and E. Tziperman, 1992: Rates of water mass formation in the North Atlantic Ocean. *J. Phys. Oceanogr.,* **22,** 93–104.

——, H.-J. Isemer, and A. Biastoch, 1995: Water mass formation from revised COADS data. *J. Phys. Oceanogr.,* **25,** 2444–2457.

Steffen, K., S. V. Nghiem, R. Huff, and G. Neumann, 2004: The melt anomaly of 2002 on the Greenland Ice Sheet from active and passive microwave satellite observations. *Geophys. Res. Lett.,* **31,** L20402, doi:10.1029/2004GL020444.

Stouffer, R. J., D. Seidov, and B. K. Haupt, 2007: Climate response to external sources of freshwater: North Atlantic versus the Southern Ocean. *J. Climate,* **20,** 436–448.

Straneo, F., 2006: Heat and freshwater transport through the central Labrador Sea. *J. Phys. Oceanogr.,* **36,** 606–628.

Tandon, A., and L. Zhao, 2004: Mixed layer transformation for the North Atlantic for 1990–2000. *J. Geophys. Res.,* **109,** C05018, doi:10.1029/2003JC002059.

Tziperman, E., 1986: On the role of interior mixing and air–sea fluxes in determining the stratification and circulation of the oceans. *J. Phys. Oceanogr.,* **16,** 680–693.

——, and K. G. Speer, 1994: A study of water mass transformation in the Mediterranean Sea: Analysis of climatological data and a simple 3-box model. *Dyn. Atmos. Oceans,* **21,** 53–82.

Vellinga, M., and R. A. Wood, 2002: Global climatic impacts of a collapse of the Atlantic thermohaline circulation. *Climatic Change,* **54,** 251–267.

Walin, G., 1982: On the relation between sea-surface heat flow and thermal circulation in the ocean. *Tellus,* **34,** 187–195.

Walsh, J. E., 1978: A data set on Northern Hemisphere sea ice extent, 1953–1976. Glaciological Data, World Data Center for Glaciology Rep. GD-2, 49–51.

Watson, R. T., D. J. Dokken, M. Noguer, P. van der Linden, C. Johnson, J. Pan, and the GRID-Arendal Design Studio Core Writing Team, Eds., 2001: *Climate Change 2001: Synthesis Report,* Cambridge University Press, 408 pp.

Weigand, H., K. U. Totsche, I. Kogel-Knabner, I. M. Belkin, S. Levitus, J. Antonov, and S.-A. Malmberg, 1998: "Great Salinity Anomalies" in the North Atlantic. *Prog. Oceanogr.,* **41,** 1–68.

Yashayaev, I., 2007: Hydrographic changes in the Labrador Sea, 1960–2005. *Prog. Oceanogr.,* **73,** 242–276.

——, M. Bersch, and H. M. van Aken, 2007: Spreading of the Labrador Sea Water to the Irminger Sea and Iceland basins. *Geophys. Res. Lett.,* **34,** L10602, doi:10.1029/2006GL028999.